ISAV	**Journal of Theoretical and Applied** **Vibration and Acoustics** journal homepage: http://tava.isav.ir	

Investigation of the efficiency of various reactive mufflers by noise reduction and transmission loss analyses

Mahya Mohammadi[a]*, Seyed Esmail Razavi[b], Cyrus Aghanajafi[c], Hadi Khorand[d]

[a] *Ph.D. Candidate, Faculty of Mechanical Engineering, K.N. Toosi University of Technology*

[b] *Professor, Faculty of Mechanical Engineering, University of Tabriz, Tabriz, Iran*

[c] *Professor, Faculty of Mechanical Engineering, K.N. Toosi University of Technology*

[d] *M.Sc., Faculty of Mechanical Engineering, University of Tabriz, Tabriz, Iran*

ARTICLE INFO

ABSTRACT

Transmission loss and noise reduction of reactive mufflers are determined by linear acoustic theory and unsteady flow field study, respectively. The effects of extending the inlet tube of the muffler, adding holes to the extension, and the number of holes on both transmission loss and noise reduction are investigated. In noise reduction analysis, the Navier-Stokes equations and k-ε model are used to study the unsteady turbulent flow. Helmholtz equation is solved for transmission loss analysis. The present study is validated with experimental data. Numerical results show a rise in noise reduction by extending the inlet tube of the muffler and increasing its length. Moreover, the extended mufflers cause more transmission loss and broadband behavior at some frequencies due to the resonances. According to the results, different points of view in the investigation of acoustic attenuation performance of mufflers can be helpful to understand more and better about the effect of geometrical parameters.

1. Introduction

Noise studies are of great importance due to their considerable effect on the human comfort. The noise of exhaust gases is one of the noise sources. The necessity of noise reduction has motivated some investigation on this issue. Silencers are used to reduce noise and they have two types: (1) active silencers and (2) passive ones[1]. Milton O. Reeves has invented the passive silencers or

---

* Corresponding author:
   E-mail address: *mahya.mohammadi@email.kntu.ac.ir* (M. Mohammadi)

mufflers[2]. Reflection of acoustic waves and absorption of sound energy are used in mufflers. Most mufflers use one of the approaches, although some of them utilize both techniques like mufflers with perforated pipes[3]. Geometric effects of mufflers on noise attenuation were studied. Nakara *et al.* [4] studied the acoustic attenuation performance of different reactive mufflers experimentally. They offered the combined mufflers to gain the high attenuation performance. Selamet and Ji[5] studied the effect of expansion chamber and extensions length and offset location of inlet and outlet ducts on acoustic attenuation performance. Lee *et al.* [6] investigated the effect of leaks from a hole in reactive silencers such as expansion chamber using 1-D transfer matrix method and experiments. They concluded that the location of the hole does not affect the transmission loss (TL) while the TL increases as the hole diameter increases at 0 frequency. Banerjee and Jacobi [7] studied the acoustic behavior of circular mufflers with single inlet/double outlet and double inlet/single outlet with different directions for inlet and outlet. They concluded that the TL of single inlet/double outlet muffler is less than the simple one because of extra transmitted energy from the additional output.

Munjal *et al.*[8] derived the differential equations for the inner and outer tube of concentric tube resonator and solved them using transfer matrix method. They found the TL of three duct muffler components. Abd EL-Rahman *et al.*[9] used a quasi-one-dimensional characteristic based non-linear model to simulate the unsteady compressible flow in concentric tube resonator. Gerges *et al.*[10] found that the transfer matrix method can be used to the primary prediction of TL. Zhu and Ji[11] found the TL of perforated reactive muffler using time domain CFD method and plane wave theory. They investigated the effect of two different boundary conditions in unsteady flow analysis to find the appropriate form of the sound pressure signal in monitoring points of inlet and outlet. Their proposed method was validated by comparing the results with experimental data. Jena and Panigrahi [12] investigated the capability of different techniques in the prediction of TL of a simple muffler with and without mean flow. They proposed suitable methods and boundary conditions for different cases of study.

Razavi *et al.* [13] investigated both fluid flow and NR in simple expansion chamber and dual one with the external connecting tube. They concluded that NR of the double chamber is more than single one while pressure loss increases somewhat.

Optimization algorithms are used in the investigation of acoustic attenuation performance of reactive mufflers, recently. Barbieri and Barbieri [14] used the FEM, then predicted the design domain, and finally evaluated the inactive elements (the elements indicating the sound hard walls) by using the genetic algorithm to improve the TL of symmetric chambers at target frequencies. Lee [15] optimized the volume and the place of rigid body elements for achieving the minimum partition volume and desirable TL at target frequency range by using the topology optimization. Ranjbar and Kermani [16] focused on the radius and length of the inlet and outlet tube and expansion chamber to modify them by Genetic algorithm and controlled random search model in order to enhance the TL. Chao and Liang[17] studied the optimization of TL and pressure drop of a reactive muffler by different algorithms and proposed the best algorithm with higher TL and less pressure drop. Azevedo *et al.*[18] used a bi-directional evolutionary acoustic topology optimization method to design the internal configuration of the single or double expansion chamber mufflers with high TL at target frequency (frequencies). Chiu *et al.* [19] studied the efficiency of genetic algorithm in conjunction with the polynomial neural network model and

boundary element model in optimizing the TL of the multi-curve tube muffler with a rectangular section within a constrained space.

Transmission loss, which is calculated by linear acoustic theory, has been studied in most research. The main contribution of this paper is to examine that plane wave theory and consequently, transmission loss analysis is accurate enough to predict the acoustic attenuation performance of mufflers or some other analyses like noise reduction are required. Investigating the TL of reactive muffler without mean flow, finding the NR of same mufflers by simulating the turbulent flow, and analyzing the performance of different reactive mufflers according to both TL and NR are studied in this study.

2. Governing Equations

There are different parameters to show the muffler performance: noise reduction, transmission loss, and insertion loss (IL). NR is the sound pressure level (SPL) difference across the muffler. IL is the sound pressure level difference at a point usually outside the system, without and with the muffler present. TL is sound power difference between the incident wave entering and transmitted wave existing muffler when the muffler is anechoic. TL is a property of muffler only and independent of sound source.

2.1. TL analysis

The Helmholtz equation is used for linearized acoustical analysis, which reads,

$$\nabla.(\frac{1}{\rho_0}\nabla p)+\frac{k^2 p}{\rho_0}=0 \quad , \quad k=2\pi f/c_0 \tag{1}$$

Where k, ρ_0, c_0, f, and p show the wavelength, fluid density, sound speed, frequency, and sound pressure, respectively. TL is defined as [20],

$$TL=10\log(\frac{W_{in}}{W_{out}}) \tag{2}$$

Where W_{in} and W_{out} denote the incoming and outgoing powers, respectively and can be calculated as an integral over the corresponding surface.

$$W_{in}=\int_{\partial\Omega}\frac{P_0^2}{2\rho c_0} \quad , \quad W_{out}=\int_{\partial\Omega}\frac{P^2}{2\rho c_0} \tag{3}$$

Eqs. (2) and (3) have been defined to COMSOL which is used for performing the TL analysis. P_0 was set to 1Pa. A is the area of the surface through which the sound power is passing.

2.2. NR analysis

According to the velocity inlet of exhaust gases (Fig. 2), the flow is incompressible and turbulent. The Reynolds-averaged Navier-Stokes equations are governed and can be written as[21],

$$\frac{\partial U_i}{\partial x_i}=0 \tag{4}$$

$$\rho \frac{\partial U_i}{\partial t} + \rho U_j \frac{\partial U_i}{\partial x_j} = -\frac{\partial p}{\partial x_i} + \frac{\partial}{\partial x_j}(2\mu S_{ji} - \overline{\rho u_j' u_i'}) \tag{5}$$

$-\overline{\rho u_j' u_i'}$ is known as the Reynolds-stress tensor and denoted by τ_{ji}. S_{ji} is the strain-rate tensor,

$$S_{ji} = \frac{1}{2}(\frac{\partial U_i}{\partial x_j} + \frac{\partial U_j}{\partial x_i}) \tag{6}$$

U_i, x_i, p, ρ, and μ are average velocity vector, position vector, pressure, density and molecular viscosity, respectively.

2.2.1. The standard k-ε turbulent model

The standard k-ε model is a semi-empirical model and obtained from the following equations[21],

$$\rho \frac{\partial k}{\partial t} + \rho U_j \frac{\partial k}{\partial x_j} = \tau_{ij}\frac{\partial U_i}{\partial x_j} - \rho \varepsilon + \frac{\partial}{\partial x_j}\left[(\mu + \mu_T/\sigma_k)\frac{\partial k}{\partial x_j}\right] \tag{7}$$

$$\rho \frac{\partial \varepsilon}{\partial t} + \rho U_j \frac{\partial \varepsilon}{\partial x_j} = C_{\varepsilon 1}\frac{\varepsilon}{k}\tau_{ij}\frac{\partial U_i}{\partial x_j} - C_{\varepsilon 2}\rho\frac{\varepsilon^2}{k} + \frac{\partial}{\partial x_j}\left[(\mu + \mu_T/\sigma_\varepsilon)\frac{\partial \varepsilon}{\partial x_j}\right] \tag{8}$$

In above equations μ_T is eddy viscosity and expressed $\rho C_\mu k^2/\varepsilon$ as . The closure coefficients are as follows,

$$C_{\varepsilon 1} = 1.44, \; C_{\varepsilon 2} = 1.92, \; C_\mu = .09, \sigma_k = 1, \sigma_\varepsilon = 1.3 \tag{9}$$

2.2.2. Fast Fourier Transform (FFT) Analysis

FFT is an algorithm that used for computing the discrete Fourier transform (DFT) and its inverse. Fourier analysis converts time to frequency and vice versa. The Fourier transform allows us to calculate the Fourier transform of a pressure signal, $p(t)$, from a finite number of its sampled points. A physical process can be depicted both in the time domain, by the values of p as a function of time, $p(t)$, or in the frequency domain, where the process is specified by giving its amplitude P as a function of frequency f, $P(f)$. By using Fourier transform equations [22],

$$P(f) = \int_{-\infty}^{\infty} p(t)e^{2\Pi ift}dt \; , \; p(t) = \int_{-\infty}^{\infty} P(f)e^{-2\Pi ift}df \tag{10}$$

The total power in a signal is the same whether it is calculated in the time domain or in the frequency domain. Using Parseval's theorem,

$$Power_{total} = \int_{-\infty}^{\infty}|p(t)|^2 dt = \int_{-\infty}^{\infty}|P(f)|^2 df \tag{11}$$

The power spectral density of the function p is as,

$$Power = 2|P(f)|^2 \tag{12}$$

$p(t)$ consists of an array of numbers i.e. a list of measurements of $p(t_i)$ for a discrete set of t_i's. Fourier transform of pressure is accounted from its sampled points. If there are N consecutive sampled values,

$$p_k = p(t_k) \ , \ t_k = k\Delta , \ k = 0,1,2,...,N-1 \qquad (13)$$

In above equation, Δ is the time interval. With N numbers of input, it is not possible to produce more than N independent numbers of output. So, instead of trying to compute the Fourier transform at all values of f, it is estimated at the discrete values,

$$f_n = \frac{n}{N\Delta}, \ n = 0,1,...,\frac{N}{2} \qquad (14)$$

The integral in Eq. (10) is estimated by a discrete summation,

$$P(f_n) = \int_{-\infty}^{\infty} P(t)e^{2\Pi i f_n t}dt = \Delta\sum_{k=0}^{N-1} p_k e^{2\Pi i kn/N} \qquad (15)$$

The summation in Eq. (15) is discrete Fourier transform of N points p_k and it is specified by P_n. Eq. (15) can be rewritten as,

$$P(f_n) = \Delta P_n \qquad (16)$$

where f_n is calculated by Eq. (14) and power spectral density is given by,

$$Power(f_0) = |p(f_0)|^2$$

$$Power(f_n) = 2|p(f_n)|^2 \ , \ n = 1,2,...,N/2 \qquad (17)$$

For each acoustic data, when the sampled data is pressure (e.g., static pressure or sound pressure), the power can be calculated using,

$$L_p(f_n) = 10\log_{10}\frac{Power(f_n)}{Power_{ref}} \quad [db], \ Power_{ref} = 4\times10^{-10}W \qquad (18)$$

where $Power(f_n)$ and $Power_{ref}$ show the power spectral density of the pressure fluctuation and the reference acoustic power, respectively.

3. Modeling and Numerical Solution Procedure

The air was chosen as working fluid. The boundary conditions of TL analysis in COMSOL consist of the incident pressure field, the interior perforated plate for perforated parts, and sound hard boundary for other boundaries. Quadratic elements were set. The damped Newton method was used for solving the equations and convergence criterion was set to 10^{-5}. Fig. 1 shows the grid configuration of the muffler with 60 mm extension in TL analysis.
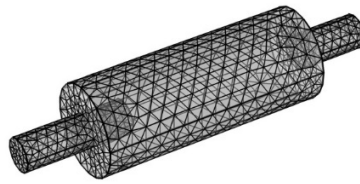
Fig 1: Grid generation of TL analysis of muffler with 60 mm extension.

The 3-D unsteady turbulent flow of exhaust gases of the A12 engine was modeled in NR analysis by ANSYS Fluent. A12 is a spark ignition engine of A series internal combustion engines of Nissan. Its technical specification is listed in Table 1. The unsteady inlet velocity of the muffler is shown in Fig. 2. The grid of simple expansion chamber and muffler with extended inlet tube was generated by hexagonal mesh and the grid of perforated parts was graded by the aid of tetrahedral mesh. The boundary conditions of NR analysis consist of velocity inlet, pressure outlet, and a series of the wall. The momentum, k and ε equations were solved by using second-order upwind and the pressure was solved by standard discretization. PISO method was used for pressure-velocity coupling. The convergence criterion and time step were set to 10^{-5} and 0.000167 *s*, respectively. The unsteady equations were solved for two crankshaft rotations at 5500 *rpm*. NR was found by FFT analysis. Fig. 3 shows the grid configuration of the muffler with 90 mm extension and 7.5% porosity in NR analysis.
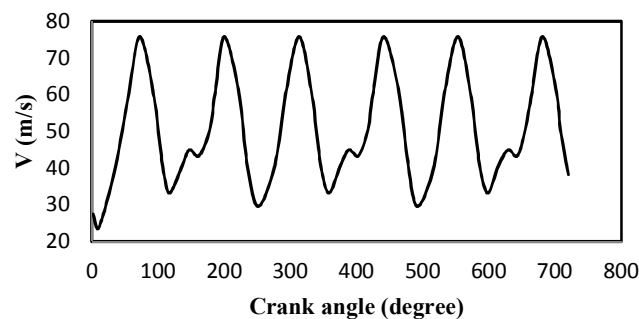
Fig 2: Inlet velocity of the muffler in NR analysis.

Table 1: Technical specification of the A12 engine.

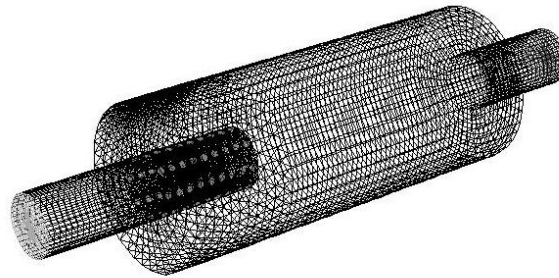| Type	inline
No. of cylinders	4
Max power	69 hp@ 6000 rpm
Max torque	94.9 N.m@ 3600 rpm
Compression ratio	9
Cylinder bore	73 mm
Stroke	70 mm
Total piston displacement	1171 cm^3
Rotation	C.C.W

130

Fig 3: Grid generation of NR analysis of muffler with 90 mm extension and 7.5% porosity.

4. Results and Discussion

Fig. 4 illustrates the cross-sectional view of studied mufflers. Table 2. shows the geometrical properties of mufflers. Figs. 5 and 6 show the mesh independent solutions of TL and NR analyses of the muffler with 60 mm extended tube and 2.5% porosity. Mesh free solution was studied for all other geometries.
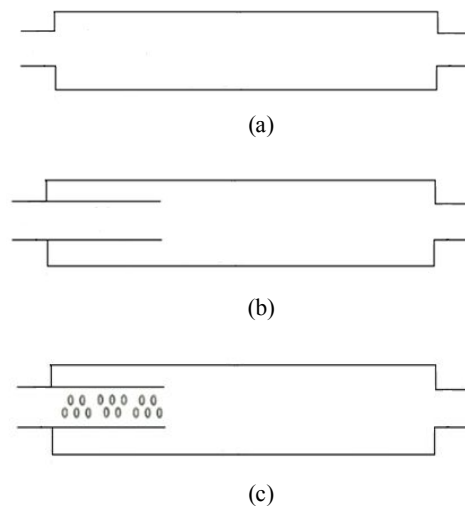

(a)

(b)

(c)

Fig 4: Cross-sectional view of studied mufflers. a) the simple expansion chamber, b) Muffler with the extended inlet tube, and c) Perforated muffler.

Table 2: Geometrical properties of mufflers.

Diameter of the expansion box	135 *mm*
Length of the expansion box	340 *mm*
Diameter of inlet and outlet tubes	50 *mm*
Length of inlet and outlet tubes	100 *mm*
Extension length	30, 60, 90 *mm*
Porosity (area ratio of perforations to that of the whole perforated plate)	2.5, 7.5 %

131
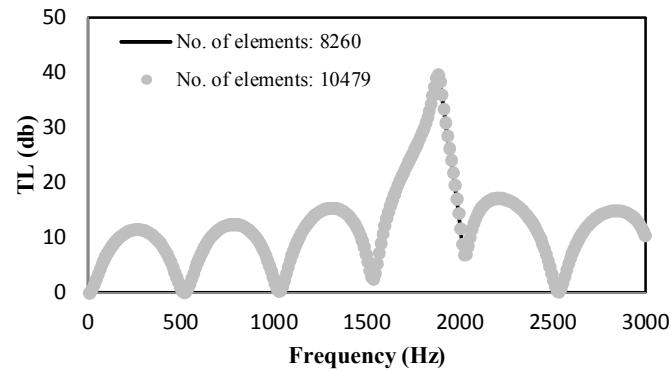
Fig 5: Grid independent solutions of TL analysis of perforated muffler with an extension length of 0.06 m and 2/5% porosity.
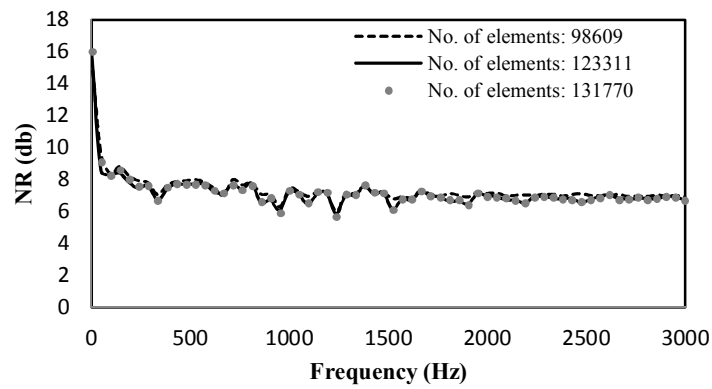
Fig 6: Grid independent solutions of NR analysis of perforated muffler with an extension length of 0.06 m and 2/5% porosity.
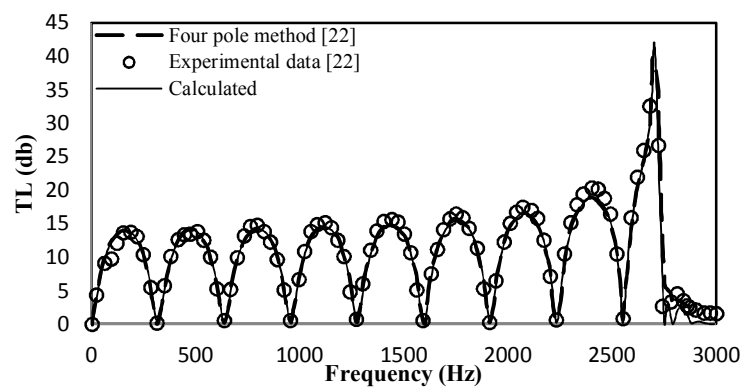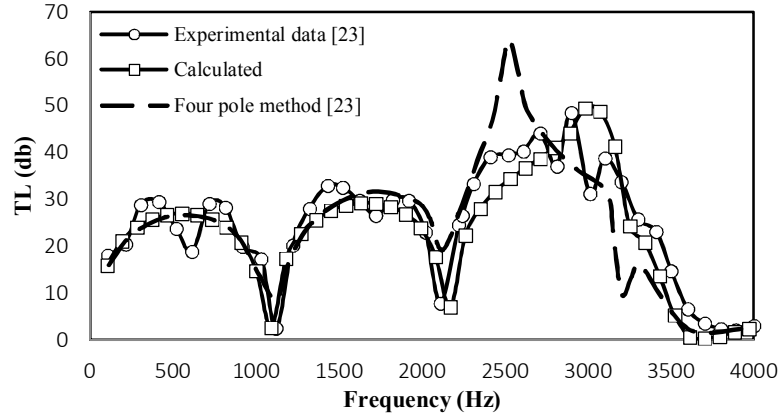
Fig 7: TL comparison between calculated result, four pole method, and published experimental one [23], Simple muffler with a length of 0.54 m and a diameter of 0.15318 m.

For validation purpose, the simulation was used for mufflers of[23] and [24]. The results were compared with published mathematical and experimental data in Figs. 7 and 8. It is shown that the difference between the present numerical result and published experimental one is negligible, so it can be concluded that the used numerical method is accurate.

Fig 8: TL comparison between calculated result, four pole method, and published experimental one [24], perforated muffler with a length of 0.16 m, a diameter of 0.118 m, and a porosity of 3.375%.

The experimental setup of published data[23] was based on the two-microphone technique. The acoustic element was between two tubes with the internal diameter of 4.859 cm. broad-frequency noise source with a signal generator module (B&k 3107) was at one end of the tube. The other end was an anechoic termination. Four $\frac{1}{4}$ *in* condenser microphones (B&k 4135) were utilized upstream and downstream of the acoustic element. The distance between the microphones in each pair was 3.556 cm. Modular multichannel analysis system (B&k 3550) was used to process the signal of microphones [23, 25].Fig. 9 shows the schematic of the experimental setup of [23]. The experimental setup of[24] is based upon the transfer function method. TL can be found by transfer function formulation, which reads,

$$TL = 20\log_{10}\left|\frac{H_r - H_{12}^u}{H_r - H_{12}^d}\right| - 20\log_{10}\left|H_t\right| + 10\log_{10}\left(\frac{A_u}{A_d}\right)$$

$$H_r = \exp(iks)$$

$$H_t = \left|\frac{S_{dd}}{S_{uu}}\right|^{1/2}$$

(19)

where H_{12}^u, H_{12}^d, S_{uu}, S_{dd}, s, A_u, and A_d denote the transfer function at the upstream, transfer function at the downstream, autospectra measured at the upstream, autospectra at the downstream, microphone spacing, inlet cross-sectional area of the muffler, and outlet cross-sectional area of the muffler. s is equal to 3.2 cm [26]. Fig. 10 shows the schematic view of the experimental setup.
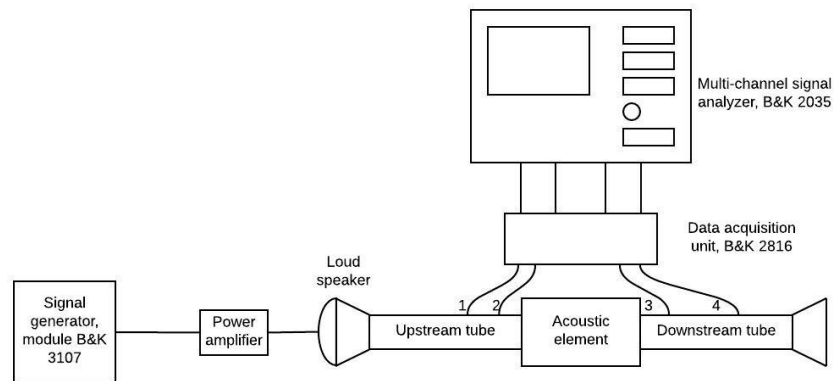
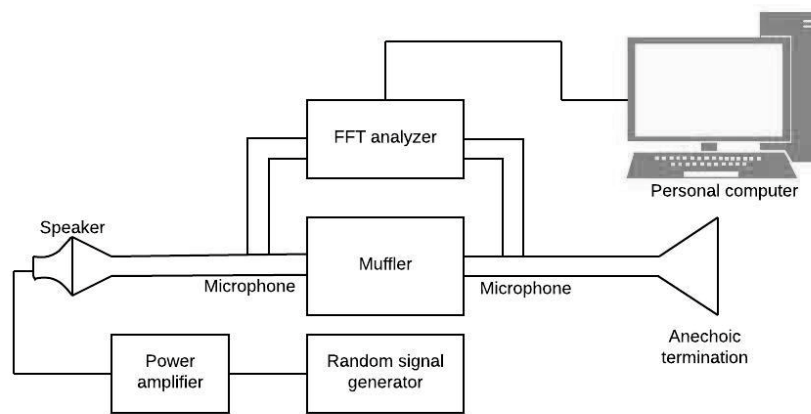**Fig 9**: The schematic of experimental setup, redrawn from [23].

Fig 10: The schematic of experimental setup, redrawn from [26].

NR and TL of the simple expansion chamber, muffler with the extended inlet tube, and perforated muffler were found. Figs. 11 and 12 show the NR and TL of the simple expansion chamber and extended muffler. According to the Fig. 11, as the inlet tube extends, some resonances occur. The number of resonances increases as the extension length increases because resonances move to the lower frequencies by increasing the resonator volume. Some broadband behavior can achieve by extending the tube and matching the resonances with the zero-attenuation frequencies similar to that in the muffler with 30 mm and 90 mm extensions. As it is seen in Fig. 12, noise reduction of the extended muffler is more than the simple expansion chamber because the SPL of inlet of muffler is more than that of the simple expansion chamber, whereas the change of SPL of outlet is negligible (according to Figs. 13 and 14). It can be concluded that extension of the tube can enhance the acoustic attenuation performance from the points of view of both NR and TL analyses.
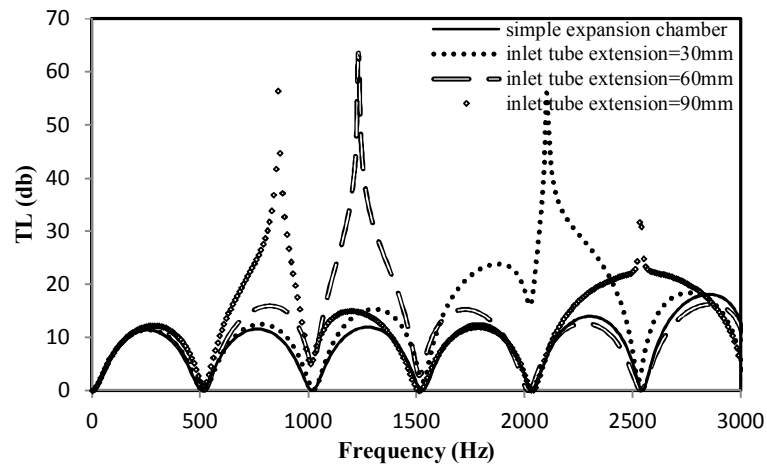
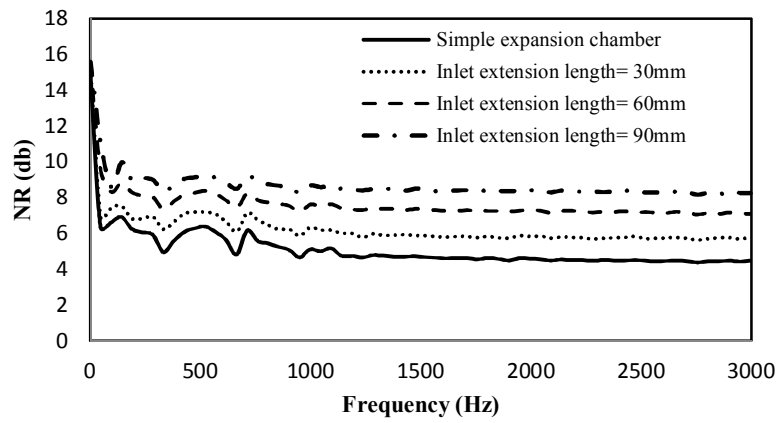**Fig 11:** TL of simple and extended mufflers.

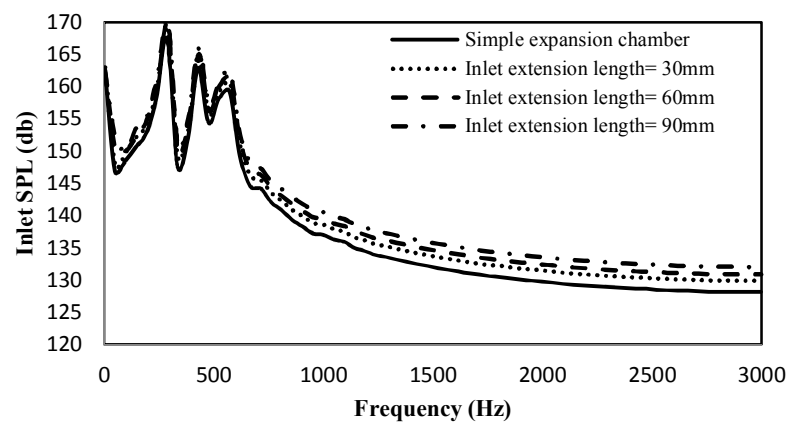**Fig 12:** NR of simple and extended mufflers.

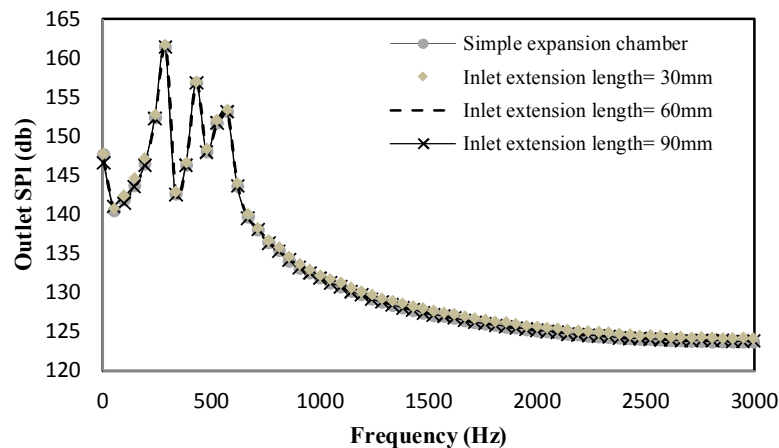**Fig 13:** Inlet SPL of simple and extended mufflers.

Fig 14: Outlet SPL of simple and extended mufflers.

Figs. 15-20 show the transmission loss and noise reduction of extended and perforated mufflers with different extension length. The location of resonances of extended mufflers moves to the higher frequencies by adding holes to the extension in TL analysis due to the dissipation of some acoustic energy. Increasing the porosity causes more sound wave attenuation entering the resonator so the high-frequency waves can be neutralized. One can use this behavior to achieve more acoustic attenuation at some target frequencies from the point of view of TL analysis. The SPL of both inlet and outlet sides of perforated muffler are higher than the extended one but the difference of SPL of the outlet is more than the SPL of the inlet (the same as in Figs. 21 and 22 for the muffler with 90 mm extension). Therefore, the NR of the perforated muffler is lower than the extended one, as it is seen in Figs. 16, 18, and 20. It is shown in Figs. 16, 18, and 20 that NR decreases as the porosity increases due to the decreasing of the SPL of inlet of muffler (the same as in Figs. 21 and 22 for the muffler with 90 mm extension). As the extension length increases, the NR difference between extended and perforated muffler increases because longer extension needs more holes in comparison to the shorter ones to have a constant porosity.
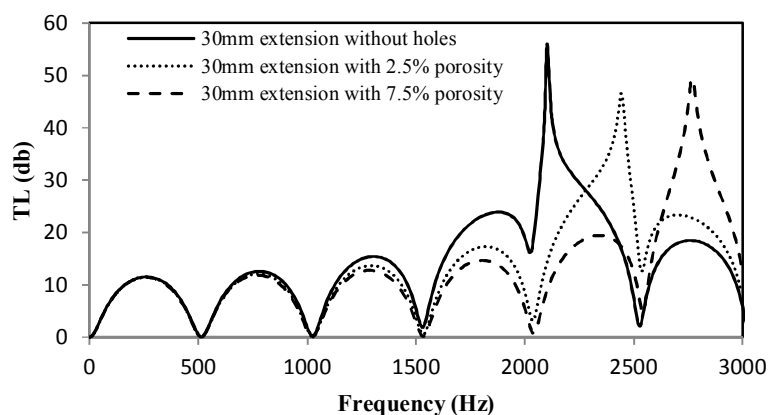

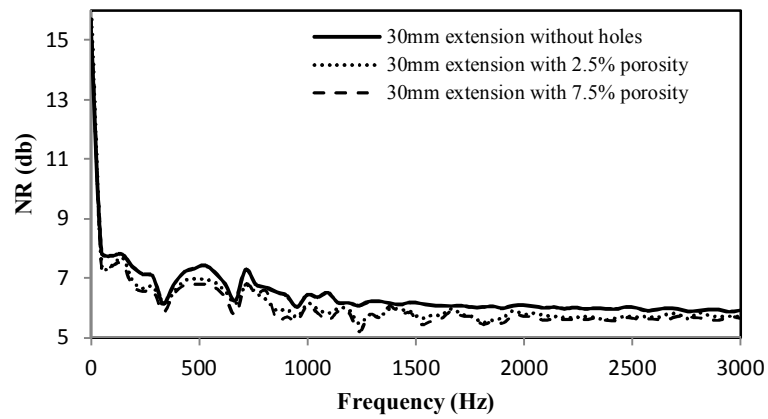**Fig 15.** TL of extended and perforated mufflers with 30 mm extension.

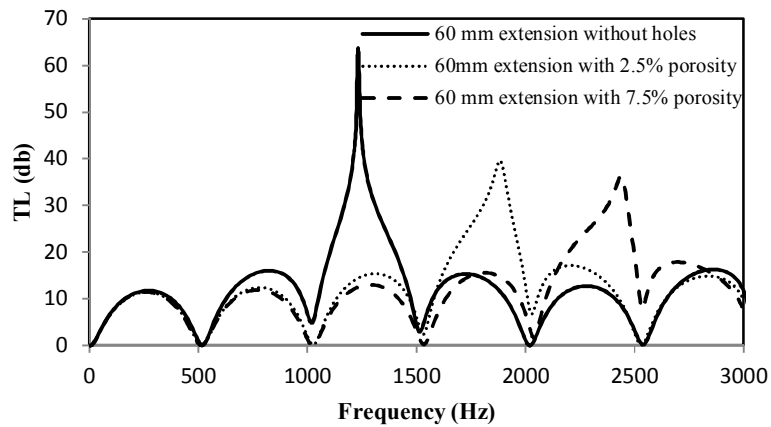**Fig 16:** NR of extended and perforated mufflers with 30 mm extension.

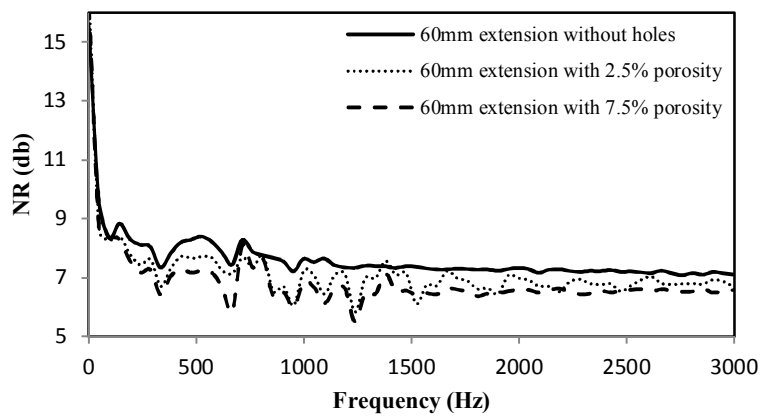**Fig 17:** TL of extended and perforated mufflers with 60 mm extension.

Fig 18: NR of extended and perforated mufflers with 60 mm extension.
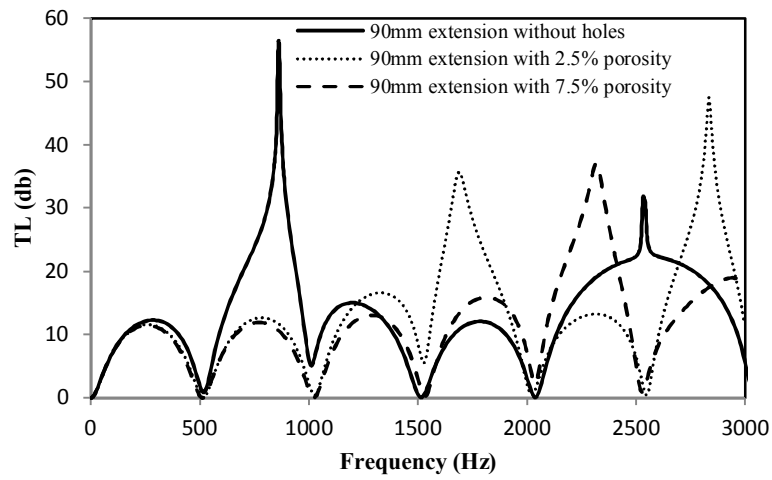
137

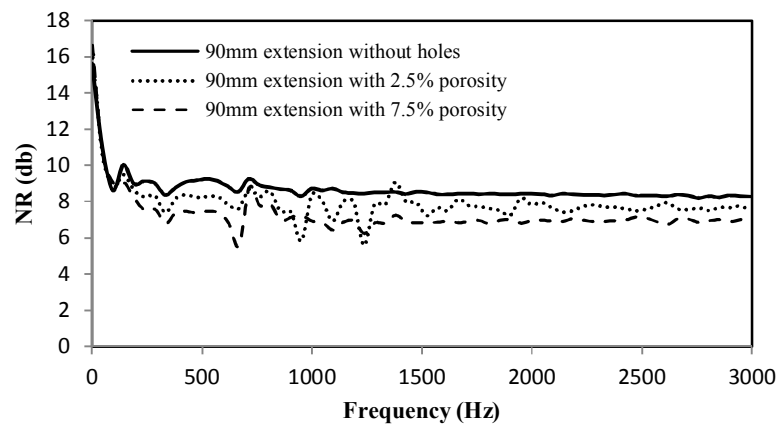**Fig 19:** TL of extended and perforated mufflers with 90 mm extension.

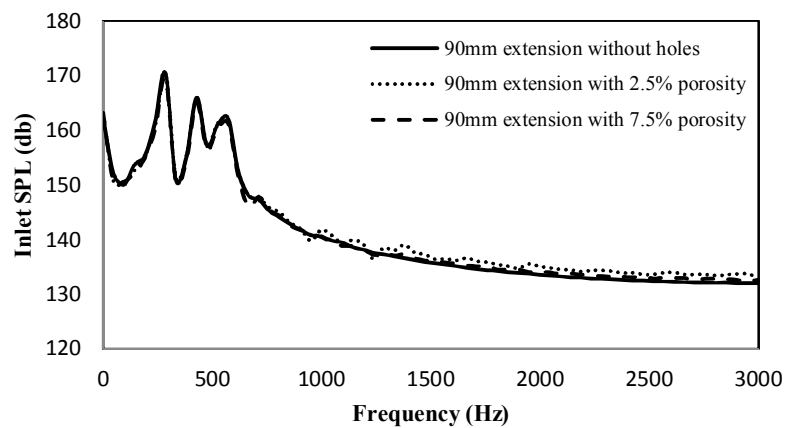**Fig 20:** NR of extended and perforated mufflers with 90 mm extension.

Fig 21. Inlet SPL of extended and perforated mufflers with 90 mm extension length.
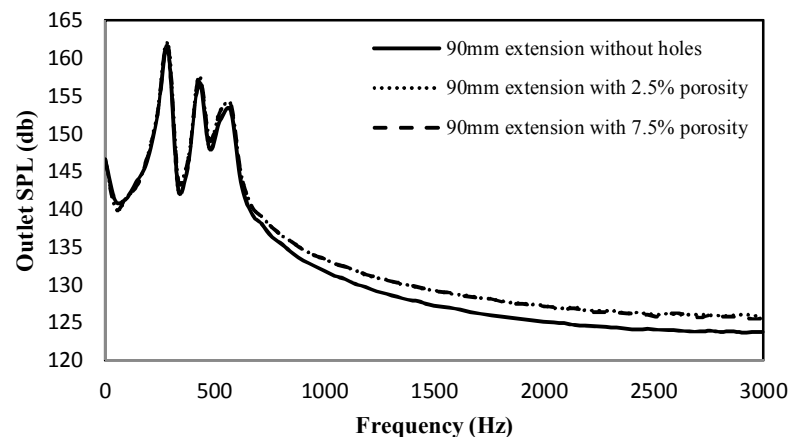
Fig 22. Outlet SPL of extended and perforated mufflers with 90 mm extension length.

5. Conclusion

In this study, the effect of some geometrical parameters of the reactive muffler on acoustical performance was studied with and without the mean flow by simulating the unsteady turbulent flow and linear plane wave propagation. Noise reduction was found by FFT method and Helmholtz equation was solved to find the transmission loss. Unsteady inlet velocity was used in NR analysis. The following results are found:

- Extending the inlet tube improves the acoustic attenuation performance of muffler according to both NR and TL analyses because the NR increases as the extension length increases and TL of muffler enhances due to some broadband behavior.

- The attenuation peak in TL analysis occurs at higher frequencies in perforated mufflers in comparison with the extended mufflers and if only the plane wave theory is taken into account, one can conclude that this behavior can be used to achieve higher acoustic attenuation performance, while the NR analysis shows another interpretation of the results.

- SPL of inlet and outlet sides of mufflers increases by adding holes to the extension and consequently the NR of perforated muffler decreases in comparison to the extended one.

- Transmission loss only depends on the geometrical parameters of the muffler while noise reduction is also a function of the flow field of the exhaust gas entering the muffler. In other words, real conditions can be considered in noise reduction analysis.

- Study of NR of mufflers along with the TL analysis seems to be useful and necessary to achieve a better perception of acoustic attenuation performance.

Refrences

[1] M.L. Munjal, Acoustics of ducts and mufflers with application to exhaust and ventilation system design, John Wiley & Sons, 1987.
[2] S. Kore, A. Aman, E. Direbsa, Performance evaluation of a reactive muffler using CFD, Journal of EEA 28 (2011) 83-89.
[3] R.F. Barron, Industrial noise control and acoustics, Marcel Dekker, Inc., New York, (2003).

[4] B.C. Nakra, W.K. Sa'id, A. Nassir, Investigations on mufflers for internal combustion engines, Applied acoustics, 14 (1981) 135-145.

[5] A. Selamet, Z.L. Ji, Acoustic attenuation performance of circular expansion chambers with extended inlet/outlet, Journal of Sound and Vibration, 223 (1999) 197-212.

[6] I. Lee, K. Jeon, J. Park, The effect of leakage on the acoustic performance of reactive silencers, Applied Acoustics, 74 (2013) 479-484.

[7] S. Banerjee, A.M. Jacobi, Transmission loss analysis of single-inlet/double-outlet (SIDO) and double-inlet/single-outlet (DISO) circular chamber mufflers by using Green's function method, Applied Acoustics, 74 (2013) 1499-1510.

[8] M.L. Munjal, K.N. Rao, A.D. Sahasrabudhe, Aeroacoustic analysis of perforated muffler components, Journal of Sound and Vibration, 114 (1987) 173-188.

[9] E.L.-R. Abd, A. I., A.S. Sabry, A. Mobarak, Non-linear simulation of single pass perforated tube silencers based on the method of characteristics, Journal of sound and vibration, 278 (2004) 63-81.

[10] S.N. Gerges, R. Jordan, F.A. Thieme, J.L. Bento Coelho, J.P. Arenas, Muffler modeling by transfer matrix method and experimental verification, Journal of the Brazilian Society of Mechanical Sciences and Engineering, 27 (2005) 132-140.

[11] D.D. Zhu, Z.L. Ji, Transmission loss prediction of reactive silencers using 3-D time-domain CFD approach and plane wave decomposition technique, Applied Acoustics, 112 (2016) 25-31.

[12] D.P. Jena, S.N. Panigrahi, Numerically estimating acoustic transmission loss of a reactive muffler with and without mean flow, Measurement, 109 (2017) 168-186.

[13] S.E. Razavi, M. Azhadarzadeh, B. Harsini, Noise Reduction in Expansion Chambers of IC Engines by Unsteady Flow Analysis, Iranian Journal of Mechanical Engineering (English) 8:, (2007) 504-515.

[14] R. Barbieri, N. Barbieri, The technique of active/inactive finite elements for the analysis and optimization of acoustical chambers, Applied Acoustics, 73 (2012) 184-189.

[15] J.W. Lee, Optimal topology of reactive muffler achieving target transmission loss values: Design and experiment, Applied acoustics, 88 (2015) 104-113.

[16] M. Ranjbar, M. Kemani, A comparative study on design optimization of mufflers by genetic algorithm and random search method, Journal of Robotic and Mechatronic Systems, 1 (2016) 7-12.

[17] s. Chao, H. Liang, Comparison of various algorithms for improving acoustic attenuation performance and flow characteristic of reactive mufflers, Applied Acoustics, 116 (2017) 291-296.

[18] F.M. Azevedo, M.S. Moura, W.M. Vicente, R. Picelli, R. Pavanello, Topology optimization of reactive acoustic mufflers using a bi-directional evolutionary optimization method, Struct Multidisc Optim, (2018) 1-14.

[19] M.C. Chiu, Y.C. Chang, H.C. Cheng, T.Y. Lin, Optimization of multiple-curve-tube mufflers using neural networks, the boundary element method and GA method, Journal of Statistics and Management Systems, 21 (2018) 787-806.

[20] F.J. Fahy, Foundations of engineering acoustics, Academic Press, Northern Illinois University, 2001.

[21] D.C. Wilcox, Turbulence modeling for CFD, DCW industries La Canada, CA, 1993.

[22] W.H. Press, B.P. Flannery, S.A. Teukolsky, W.T. Vetterling, Numerical recipes, Cambridge university press Cambridge, 1989.

[23] A. Selamet, P.M. Radavich, The effect of length on the acoustic attenuation performance of concentric expansion chambers: an analytical, computational and experimental investigation, Journal of Sound and Vibration, 201 (1997) 407-426.

[24] C.N. Wang, A numerical scheme for the analysis of perforated intruding tube muffler components, Applied Acoustics, 44 (1995) 275-286.

[25] A. Selamet, N. Dickey, J. Novak, The Herschel–Quincke tube: a theoretical, computational, and experimental investigation, The Journal of the Acoustical Society of America, 96 (1994) 3177-3185.

[26] C.N. Wang, C.C. Tse, Y.N. Chen, Analysis of three dimensional muffler with boundary element method, Applied acoustics, 40 (1993) 91-106.